Nuclear Spin Dynamics, Noise, Squeezing, and Entanglement in Box Model

A. V. Shumilin and D. S. Smirnov*
Ioffe Institute, 194021 St. Petersburg, Russia

(Received 9 December 2020; revised 24 March 2021; accepted 27 April 2021; published 27 May 2021)

We obtain a compact analytical solution for the nonlinear equation for the nuclear spin dynamics in the central spin box model in the limit of many nuclear spins. The total nuclear spin component along the external magnetic field is conserved and the two perpendicular components precess or oscillate depending on the electron spin polarization, with the frequency, determined by the nuclear spin polarization. As applications of our solution, we calculate the nuclear spin noise spectrum and describe the effects of nuclear spin squeezing and many body entanglement in the absence of a system excitation.

DOI: 10.1103/PhysRevLett.126.216804

Introduction.—The problem involving a single "central" spin interaction with surrounding spins is known as the central spin model. It is widely used to describe the interaction of a localized electron with nuclei, for example, in quantum dots or in the vicinity of donors in bulk semiconductors [1]. Generally, this is a complex many body problem, and it has been studied in detail [2,3]. In particular, the central spin model allows one to describe the Hanle effect in a transverse magnetic field [4], polarization recovery in a longitudinal field [5,6], spin precession mode locking [7], nuclei-induced frequency focusing [8], spin noise [9–11], the effect of spin inertia [12,13], dynamic nuclear spin polarization [14], and many other effects.

Interest in the intertwined electron and nuclear spin dynamics is driven mostly by the perspective of quantum dot based scalable technology for quantum computations [15–17]. Most previous studies considered the nuclear spins as an important source of electron spin decoherence [18–20]. But recently the nuclear spins were recognized as a possible platform for quantum information storage and processing [21,22]. For example, a coherent interface between electron and nuclear spins was developed [23], sensing of single quantum nuclear spin excitation was realized [24], and elementary quantum algorithms were implemented in the nuclear spin quantum register in strained quantum dots [25].

The complexity of the nuclear spin dynamics is related mainly to the large number of nuclei interacting with a single electron. Despite the possibility of diagonalizing the central spin model Hamiltonian for a finite number of nuclei using the Bethe ansatz [26] and of calculating the nuclear spin dynamics in the box model [27–29], it is still hardly possible to qualitatively describe the nuclear spin dynamics, especially for many nuclear spins [30–32]. In this Letter we solve this long-standing problem and obtain the exact expressions for the nuclear spins dynamics in the limit of many nuclear spins. These expressions are used to calculate the nuclear spin noise spectra, and to describe the effects of intrinsic nuclear spin squeezing and many body entanglement in the central spin model.

Nuclear spin dynamics in the box model.—The Hamiltonian of the box model has the form

$$\mathcal{H} = A\boldsymbol{I}\boldsymbol{S} + \hbar\boldsymbol{\Omega}_B\boldsymbol{S} + \hbar\boldsymbol{\omega}_B\boldsymbol{I}, \tag{1}$$

where A is the constant of the hyperfine coupling between the total nuclear spin $\boldsymbol{I}$ and the electron spin $\boldsymbol{S}$, and $\boldsymbol{\Omega}_B$ and $\boldsymbol{\omega}_B$ are electron and nuclear spin precession frequencies in the external magnetic field, respectively. Throughout the Letter we use the minuscule and majuscule omegas to denote the nuclear and electron spin precession frequencies, respectively. The total nuclear spin is composed of N individual nuclear spins $\boldsymbol{I}_n$: $\boldsymbol{I} = \sum_{n=1}^{N}\boldsymbol{I}_n$. Thus, the box model is a particular case of the central spin model where all the hyperfine coupling constants are equal.

In the Heisenberg representation the electron spin operator obeys the Bloch equation

$$\frac{d\boldsymbol{S}}{dt} = \boldsymbol{\Omega}_e \times \boldsymbol{S}, \tag{2}$$

where $\boldsymbol{\Omega}_e = \boldsymbol{\Omega}_B + \boldsymbol{\Omega}_N$ is the total electron spin precession frequency and $\boldsymbol{\Omega}_N = A\boldsymbol{I}/\hbar$ is the frequency related to the Overhauser field. Thus, the electron spin rotates in the sum of the nuclear and external magnetic fields, as illustrated in Fig. 1(a).

Similarly, the nuclear spin operator obeys

$$\frac{d\boldsymbol{I}}{dt} = \left(\frac{A}{\hbar}\boldsymbol{S} + \boldsymbol{\omega}_B\right) \times \boldsymbol{I}. \tag{3}$$

One can see that the system states with the different absolute values of the total nuclear spin I are not mixed, so it is a good quantum number.

Generally, one cannot replace the operators $\boldsymbol{S}$ and $\boldsymbol{I}$ in Eqs. (2) and (3) with their average values and solve the

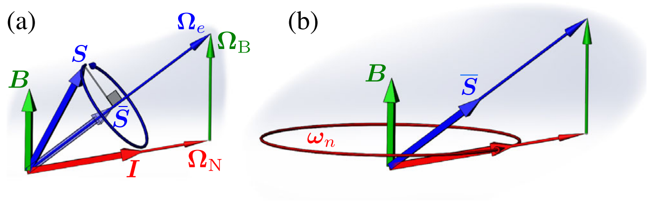

FIG. 1. (a) Electron spin precesses around the sum of the external magnetic field and the Overhauser field and effectively projects in the direction of $\mathbf{\Omega}_e$. (b) At long timescales the average electron spin adiabatically follows the direction of $\mathbf{\Omega}_e$ and induces the nuclear spin precession around the direction of the magnetic field with the frequency $\boldsymbol{\omega}_n$.

resulting equations. This procedure would give, for example, no effect of the hyperfine interaction for the nuclear spin dynamics if the electron spin were unpolarized, which is not correct because of the quantum uncertainty for electron spin, which is as large as its maximum possible average value. This problem was solved previously only numerically. Below we solve it analytically in the limit of a large nuclear spin.

In self-assembled GaAs quantum dots, typically, $N \sim 10^5$, so even in the absence of nuclear spin polarization the typical fluctuation of $I \sim \sqrt{N}$ is very large. Note also that the nuclear magnetic moment is much smaller than that of an electron, so we assume that $\omega_B \ll \Omega_B$. In this case the electron spin precession is much faster than that of the nuclei [18], which allows us to find the compact exact solution.

Formally, the solution of Eq. (2) is $\boldsymbol{S}(t) = e^{i\mathcal{H}t/\hbar}\boldsymbol{S}e^{-i\mathcal{H}t/\hbar}$. For large nuclear spin $I \gg 1$ we shall neglect the commutator of its components hereafter [33] [it was not neglected in the derivation of Eq. (3) for the only time], which yields $\boldsymbol{S}(t) = e^{i\mathbf{\Omega}_e\boldsymbol{S}t}\boldsymbol{S}e^{-i\mathbf{\Omega}_e\boldsymbol{S}t}$. The standard decomposition of the spin matrix exponents gives

$$\boldsymbol{S}(t) = \left[\cos(\Omega_e t/2) + 2i\frac{\boldsymbol{S}\mathbf{\Omega}_e}{\Omega_e}\sin(\Omega_e t/2)\right]\boldsymbol{S} \times \left[\cos(\Omega_e t/2) - 2i\frac{\boldsymbol{S}\mathbf{\Omega}_e}{\Omega_e}\sin(\Omega_e t/2)\right]. \quad (4)$$

Note that $\mathbf{\Omega}_e$ here is still an operator. In fact this expression contains only the even powers of Ω_e, which can be calculated as $\Omega_e^2 = \mathbf{\Omega}_e^2$.

Equation (4) contains oscillating terms and has a nonzero time average

$$\bar{\boldsymbol{S}} = \frac{\mathbf{\Omega}_e(\mathbf{\Omega}_e\boldsymbol{S})}{\Omega_e^2}. \quad (5)$$

It has the meaning of the projection of the electron spin on the direction of $\mathbf{\Omega}_e$ [18], as illustrated in Fig. 1(a). Note that $\bar{\boldsymbol{S}}$ is an operator and not a quantum mechanical average.

In view of the separation of the timescales of the electron and nuclear spin dynamics, the electron spin in Eq. (3) can be replaced with its average:

$$\frac{d\boldsymbol{I}}{dt} = \left(\frac{A}{\hbar}\bar{\boldsymbol{S}} + \boldsymbol{\omega}_B\right) \times \boldsymbol{I}. \quad (6)$$

It is convenient to rewrite this equation as

$$\frac{d\boldsymbol{I}}{dt} = \frac{A}{\hbar}\boldsymbol{e}_z \times \boldsymbol{J} + \boldsymbol{\omega}_B \times \boldsymbol{I}, \quad (7)$$

where $\boldsymbol{J} = (\mathbf{\Omega}_e\boldsymbol{S})\Omega_B\boldsymbol{I}/\Omega_e^2$ describes the correlation between electron and nuclear spins and $\boldsymbol{e}_z$ is the unit vector along the $\mathbf{\Omega}_B$ direction. This is an auxiliary quantity. For example, in a strong magnetic field $\mathbf{\Omega}_e \approx \mathbf{\Omega}_B$, so $\boldsymbol{J} = \boldsymbol{I}S_z$, which has a clear meaning for the electron and nuclear spin correlators.

We note that $\mathcal{H} \approx \mathbf{\Omega}_e\boldsymbol{S}$, so this product is constant, which can be referred to as the adiabatic approximation. Moreover, $\mathcal{H}^2 \approx \Omega_e^2/4$, so Ω_e^2 is also constant. Therefore, using Eq. (3) we obtain

$$\frac{d\boldsymbol{J}}{dt} = \frac{A}{\hbar}\frac{\Omega_B^2}{4\Omega_e^2}\boldsymbol{e}_z \times \boldsymbol{I} + \boldsymbol{\omega}_B \times \boldsymbol{J}. \quad (8)$$

This equation along with Eq. (7) forms a closed set. It accounts for the electron spin commutation relations but neglects the nuclear ones. This set is exact in the limit of large I, and that is the main result of this Letter.

Quasiclassical interpretation.—In Eqs. (7) and (8) all the quantities (except for $\mathbf{\Omega}_B$ and $\boldsymbol{\omega}_B$) are operators. In this section we replace all the operators with their average values but use the same notations for brevity.

It is convenient to rewrite Eqs. (7) and (8) for the quantum mechanical average values in more physically transparent notations. The direction of $\mathbf{\Omega}_e$ represents a good electron spin quantization axis, so the quantities $P_\pm = 1/2 \pm \mathbf{\Omega}_e\boldsymbol{S}/\Omega_e$ represent the probabilities of the electron spin being parallel or antiparallel to this direction. We also introduce

$$\boldsymbol{I}^\pm = \left(\frac{\boldsymbol{I}}{2} \pm \frac{\Omega_e}{\Omega_B}\boldsymbol{J}\right)/P_\pm, \quad (9)$$

which represent the nuclear spins in these two cases, respectively. Importantly, one should use the average value $\boldsymbol{J}$ here and should not replace it with the product of the average values from the definition in order to correctly describe the correlations between electron and nuclear spins. The total nuclear spin is given by $\boldsymbol{I} = P_+\boldsymbol{I}^+ + P_-\boldsymbol{I}^-$.

From Eqs. (7) and (8) we simply obtain

$$\frac{d\boldsymbol{I}^\pm}{dt} = \boldsymbol{\omega}_n^\pm \times \boldsymbol{I}^\pm, \quad (10)$$

where

$$\boldsymbol{\omega}_n^\pm = \pm\omega_e \frac{\boldsymbol{\Omega}_B}{\Omega_e} + \boldsymbol{\omega}_B, \tag{11}$$

with $\omega_e = A/(2\hbar)$ being the nuclear spin precession frequency in the Knight field of completely spin polarized electron. Thus, in the cases of electron spin parallel or antiparallel to $\boldsymbol{\Omega}_e$, the total nuclear spin precesses with the frequency $\boldsymbol{\omega}_n^\pm$, respectively. This is illustrated in Fig. 1(b). The external magnetic field tilts the average electron spin $\bar{\boldsymbol{S}}$ from the direction of $\boldsymbol{\Omega}_N$ to $\boldsymbol{\Omega}_e$. As a result, the Knight field being parallel to $\bar{\boldsymbol{S}}$ tilts from the direction of $\boldsymbol{I}$ and leads to the nuclear spin precession [34]. However, this precession is slow, so the electron spin adiabatically follows the direction of $\boldsymbol{\Omega}_e$. In this case the Knight, the Overhauser and external magnetic fields always lie in one plane, so the nuclear spin rotates around the z axis with the frequency $\boldsymbol{\omega}_n^\pm$. The total nuclear spin dynamics represents the superposition of precessions with these two frequencies.We stress that due to the dependence of $\boldsymbol{\omega}_n^\pm$ on $\boldsymbol{\Omega}_N$, Eqs. (10) describing the nuclear spin dynamics are formally nonlinear.

The solution of Eqs. (10) in the case of $\omega_B = 0$ yields

$$I_x(t) = I_x(0)\cos(\omega_n t) - \frac{2(\boldsymbol{\Omega}_e \boldsymbol{S})}{\Omega_e} I_y(0)\sin(\omega_n t), \tag{12a}$$

$$I_y(t) = I_y(0)\cos(\omega_n t) + \frac{2(\boldsymbol{\Omega}_e \boldsymbol{S})}{\Omega_e} I_x(0)\sin(\omega_n t), \tag{12b}$$

where $\omega_n = |\boldsymbol{\omega}_n^\pm|$ (note that $\boldsymbol{\Omega}_e \boldsymbol{S}$ and Ω_e do not depend on time). Crucially, these expressions demonstrate that the nuclear spin oscillates even in the absence of electron spin polarization ($\bar{\boldsymbol{S}} = 0$) due to the electron spin quantum uncertainty. In this case the superposition of the two precessions in the Knight field with the opposite frequencies results in the nuclear spin oscillations, while $\omega_B = 0$.

We have checked to ensure that our theory agrees with the numerical solution of the Schrödinger equation with the accuracy $\propto 1/N$ [35].

Nuclear spin noise.—Nuclear spin dynamics can be most easily studied experimentally in close to equilibrium conditions through its action on the electron. In this case it is characterized by the nuclear spin noise spectra [11,39]

$$(I_\alpha^2)_\omega = \int_{-\infty}^{\infty} \langle I_\alpha(t) I_\alpha(t+\tau)\rangle e^{i\omega\tau} d\tau, \tag{13}$$

where the angular brackets denote the statistical averaging. These spectra can be measured directly using the resonance shift spin noise spectroscopy [40,41]. In the steady state the correlator in the integrand does not depend on t. Its dependence on τ is given by the solution of Eq. (10), which should be averaged over the initial conditions taken from the equilibrium nuclear spin distribution function.

The noise spectrum of the transverse spin components reads [35]

$$(I_x^2)_\omega = \sum_\pm \frac{\sqrt{\pi}\delta^3}{16\omega_\pm^3 \Omega_B} \exp\left[-\left(\frac{\Omega_B}{\delta}\right)^2 \left(\frac{\omega_e^2}{\omega_\pm^2} + 1\right)\right] \times \left[\frac{2\omega_e \Omega_B^2}{\omega_\pm \delta^2} \mathrm{ch}\left(\frac{2\omega_e \Omega_B^2}{\omega_\pm \delta^2}\right) - \mathrm{sh}\left(\frac{2\omega_e \Omega_B^2}{\omega_\pm \delta^2}\right)\right] \tag{14}$$

and $(I_y^2)_\omega = (I_x^2)_\omega$. Here δ is the typical fluctuation of Ω_N ($\langle \Omega_N^2 \rangle = 3\delta^2/2$) and $\omega_\pm = \omega \pm \omega_B$. This result agrees with the numerical calculations performed in Ref. [39]. The nuclear spin noise spectrum is shown in Fig. 2 as solid curves for the case of zero nuclear g factor ($\omega_B = 0$). Generally, the spectrum is an even function of ω, so the positive frequencies only are shown in the figure. The spectrum consists of a single peak, which shifts from $\omega = 0$ to $\omega = \omega_e$ with an increase of the magnetic field. Its width changes nonmonotonously: it vanishes in the limits of weak and strong magnetic fields, and it is of the order of ω_e when $\Omega_B \sim \delta$; the width of the peak is of the order of its central frequency in this case.

The shift of the peak in the spin noise spectrum with an increase of the magnetic field is related to the acceleration of the nuclear spin precession in the Knight field. In a small magnetic field, the electron spin is almost parallel to the nuclear spin, so it hardly causes the nuclear spin precession. However, the stronger the magnetic field, the larger the deviation of the average electron spin $\bar{\boldsymbol{S}}$ from the direction of the total nuclear spin $\boldsymbol{I}$, and the faster the nuclear spin precession. In the limit of a strong magnetic field, the electron spin is parallel to it, which leads to the precession of the transverse nuclear spin components with the frequency ω_e (in the case of $\omega_B = 0$). Hence, the nuclear spin noise spectrum is centered around this frequency [39]. The

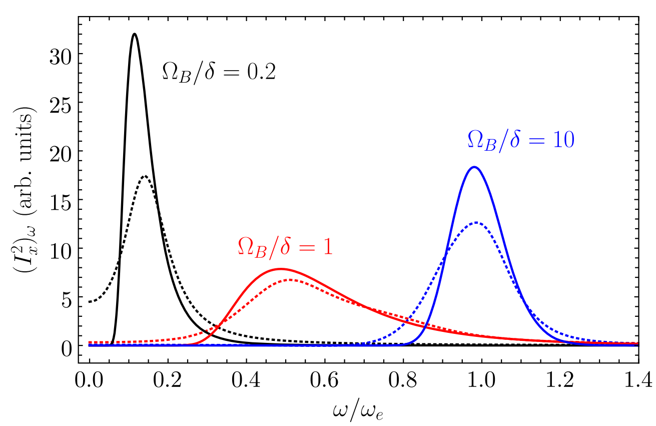

FIG. 2. Nuclear spin noise spectra calculated after Eq. (14) for different strengths of the magnetic field indicated by the labels, neglecting the nuclear Zeeman splitting, $\omega_B = 0$. The dotted curves are calculated for the same parameters with the addition of the nuclear spin relaxation time $\tau_s^n \omega_e = 25$ [35].

finite nuclear g factor leads to the splitting of the peaks at both negative and positive frequencies [35].

The effect of the electron, τ_s^e, and nuclear, τ_s^n, spin relaxation times can be described using the kinetic equations for the distribution functions of $\boldsymbol{I}^\pm$ [35]. The effect of τ_s^n is illustrated in Fig. 2 by the dotted curves. The nuclear spin relaxation generally broadens the spectra. In particular, in weak ($\Omega_B \tau_s^n \omega_e / \delta \ll 1$) and strong ($\Omega_B / \delta \gg 1$) magnetic fields the spectrum represents a Lorentzian at $\omega = 0$ and $\omega = \omega_e$, respectively, with the width $1/\tau_s^n$. Moreover, if the nuclear spin relaxation is fast, $\tau_s^n \omega_e \ll 1$, the spectrum is always Lorentzian centered at zero frequency, having the large width $1/\tau_s^n$.

Nuclear spin squeezing and entanglement.—As another important application, we describe the squeezing of the nuclear spin distribution function [42]. The spin squeezing is currently being widely studied [43–46], mainly in the field of quantum metrology, as it allows one to increase the phase sensitivity in the Ramsey interferometry beyond the standard quantum limit [47]. In applications to quantum dots it can also be used to increase the electron spin coherence time [48,49]. Previously, it was suggested that the nuclear spin squeezing can be produced by the quadrupole interaction [50] or in the presence of external driving under the conditions of fast electron spin relaxation [48].

Our solution of the nuclear spin dynamics predicts the dependence of the nuclear spin precession frequency on its value, Eq. (11). Therefore, after the preparation of the coherent nuclear spin state with the average polarization being perpendicular to the external magnetic field (say, along the x axis) and electron spin polarization along $\boldsymbol{\Omega}_e$ [35], different spins in the distribution precess at different frequencies. This produces the nuclear spin squeezing *intrinsically* in the central spin model. An example of the squeezed nuclear spin distribution produced in this way is given in the inset of Fig. 3(a).

The distribution squeezing is described by the parameter ξ_S [51], which is the ratio of the minimal spin standard deviation over the directions perpendicular to the average spin and its value for the coherent spin state [35]. This is shown in Fig. 3(a) as a function of time for the different nuclear spin polarization degrees, P. One can see that the larger the polarization, the faster ξ_S decreases, but the sooner it saturates. In typical GaAs based quantum dots, $\omega_e \sim 1\ \mu\text{s}^{-1}$ and spin relaxation time $\tau_s^n \sim 0.1$ ms, so $\omega_e \tau_s^n \sim 100$ and very strong nuclear spin squeezing, $\xi_S \sim 10^{-2}$, can be reached.

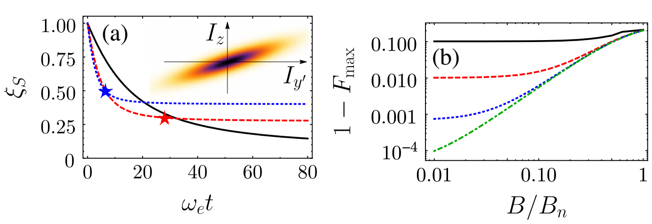

FIG. 3. (a) Degree of the nuclear spin squeezing, ξ_S, as a function of free nuclear spin precession time for the nuclear spin polarization $P = 10\%$ (black solid curve), 30% (red dashed curve), and 50% (blue dotted curve). Inset: nuclear spin distribution in the plane perpendicular to the average spin at the time marked with the blue star. The external magnetic field is equal to the average nuclear field, $\Omega_B = |\langle \boldsymbol{\Omega}_N \rangle|$ and $N = 10^6$. (b) Infidelity of GHZ state preparation as a function of the applied magnetic field $B/B_n = \Omega_B/\Omega_N$ for $N = 6$ (black solid curve), 80 (red dashed curve), 1200 (blue dotted curve), and 2×10^4 (green dot-dashed curve).

The interferometry beyond the standard quantum limit requires the metrological degree of the spin squeezing $\xi_R = \xi_S / P$ to be less than unity [52]. This criterion is more difficult to satisfy, and for $P = 10\%$ it is not reached. However, for larger nuclear spin polarizations it is reached at the points marked by the red and blue stars in Fig. 3(a). Since in modern experiments a polarization of up to 80% is feasible [53], we believe that the metrological nuclear spin squeezing can be obtained as well.

Spin squeezing evidences the nuclear spin entanglement [47]. In the central spin model it is produced by the indirect interaction between nuclei mediated by the electron spin. While there are a number of entanglement measures [54], an example of the maximally entangled state is the Greenberger-Horne-Zeilinger (GHZ) state, which is a coherent superposition of collective spin states pointing in opposite directions. To approach this state, we suggest orienting the electron spin in the direction which is perpendicular to both the initial nuclear spin direction and the external magnetic field (say, the y axis) [35]. In this case the good electron spin quantization axis is perpendicular to it, so the nuclear spin dynamics represents the coherent superposition of precessions with the frequencies $\boldsymbol{\omega}_n^\pm$; see Eqs. (12). After the relative phase $(\omega_n^+ - \omega_n^-)t$ reaches π, the nuclear spin state is close to the GHZ state.

The infidelity [47,54] of the GHZ state preparation is shown in Fig. 3(b) as a function of the magnetic field for different numbers of nuclei. It decreases with a decrease of the magnetic field and an increase of the number of nuclei, but it is generally very low. However, the smaller the magnetic field, the slower the increase of the relative phase. Since the preparation time should be below τ_s^n, one has to consider $B/B_n \gtrsim 10^{-2}$, which still produces very high fidelity of up to 99.99%.

We note also that since the nuclear spin polarization produces macroscopic magnetic fields of the order of a few tesla, the nuclear GHZ state would be a coherent superposition of the macroscopically different states, known as a Schrödinger cat state [55]. Such states are important for quantum metrology and investigations of the quantum-classical correspondence [56–58].

Discussion and conclusion.—The box model considered in this Letter is known to also give qualitatively correct results for the general central spin model [59–62]. For example, the nuclear spin noise spectra for homogeneous and inhomogeneous hyperfine coupling are very similar [39]. The most important deviations are expected in the nuclear spin squeezing and entanglement, as the different nuclear spins would precess at different frequencies for the inhomogeneous hyperfine coupling. However, the nuclear spin precession frequency would be almost the same in a central core of the electron wave function, which can include hundreds of nuclei. Thus, a high degree of spin squeezing and entanglement is expected for these core spins.

The nuclear spin dynamics calculated in this Letter is important for nuclear spin based quantum computations, as well as for the description of the optical properties of single quantum dots [63,64] and the transport properties of double quantum dots in the spin blockade regime [65]. For example, the nuclear spin precession probably explains the low frequency peaks in the electron spin noise spectra predicted in the numerical simulations [66]. Another application is related with organic semiconductors, where the hyperfine interaction determines the optical and electrical properties even at room temperature [67–69]. We address this specific issue in a joint paper [70].

In summary, in this Letter we derived the exact nonlinear equations for the nuclear spin dynamics and obtained their compact solution in the box model with many nuclear spins. It was used to calculate the nuclear spin noise spectra, and to describe the effects of nuclear spin squeezing and many body entanglement, which take place intrinsically after preparation of the appropriate coherent nuclear spin state. We believe that our results will be useful for descriptions of the electron and nuclear spin dynamics for the localized electrons in various nanostructures and under different experimental conditions.

We gratefully acknowledge the fruitful discussions with M. M. Glazov and the partial financial support from RF President Grant No. MK-1576.2019.2 and the Foundation for the Advancement of Theoretical Physics and Mathematics "Basis." We also thank S. G. Smirnov for the design of Fig. 1. The calculation of the nuclear spin dynamics by D. S. S. was supported by Russian Science Foundation Grant No. 19-12-00051. A. V. S. acknowledges support from Russian Foundation for Basic Research Grant No. 19-02-00184.

[*]smirnov@mail.ioffe.ru

[1] M. M. Glazov, *Electron and Nuclear Spin Dynamics in Semiconductor Nanostructures* (Oxford University Press, Oxford, 2018).

[2] W. A. Coish and J. Baugh, Nuclear spins in nanostructures, Phys. Status Solidi B **246**, 2203 (2009).

[3] W. Yang, W.-L. Ma, and R.-B. Liu, Quantum many-body theory for electron spin decoherence in nanoscale nuclear spin baths, Rep. Prog. Phys. **80**, 016001 (2017).

[4] Y. G. Semenov and K. W. Kim, Effect of an external magnetic field on electron-spin dephasing induced by hyperfine interaction in quantum dots, Phys. Rev. B **67**, 073301 (2003).

[5] P.-F. Braun, X. Marie, L. Lombez, B. Urbaszek, T. Amand, P. Renucci, V. K. Kalevich, K. V. Kavokin, O. Krebs, P. Voisin, and Y. Masumoto, Direct Observation of the Electron Spin Relaxation Induced by Nuclei in Quantum Dots, Phys. Rev. Lett. **94**, 116601 (2005).

[6] D. S. Smirnov, E. A. Zhukov, D. R. Yakovlev, E. Kirstein, M. Bayer, and A. Greilich, Spin polarization recovery and Hanle effect for charge carriers interacting with nuclear spins in semiconductors, Phys. Rev. B **102**, 235413 (2020).

[7] I. A. Yugova, M. M. Glazov, D. R. Yakovlev, A. A. Sokolova, and M. Bayer, Coherent spin dynamics of electrons and holes in semiconductor quantum wells and quantum dots under periodical optical excitation: Resonant spin amplification versus spin mode locking, Phys. Rev. B **85**, 125304 (2012).

[8] A. Greilich, A. Shabaev, D. R. Yakovlev, Al. L. Efros, I. A. Yugova, D. Reuter, A. D. Wieck, and M. Bayer, Nuclei-induced frequency focusing of electron spin coherence, Science **317**, 1896 (2007).

[9] M. M. Glazov and E. L. Ivchenko, Spin noise in quantum dot ensembles, Phys. Rev. B **86**, 115308 (2012).

[10] N. A. Sinitsyn, Yan Li, S. A. Crooker, A. Saxena, and D. L. Smith, Role of Nuclear Quadrupole Coupling on Decoherence and Relaxation of Central Spins in Quantum Dots, Phys. Rev. Lett. **109**, 166605 (2012).

[11] D. S. Smirnov, V. N. Mantsevich, and M. M. Glazov, Theory of optically detected spin noise in nanosystems, Phys. Usp. (2021).

[12] F. Heisterkamp, E. A. Zhukov, A. Greilich, D. R. Yakovlev, V. L. Korenev, A. Pawlis, and M. Bayer, Longitudinal and transverse spin dynamics of donor-bound electrons in fluorine-doped ZnSe: Spin inertia versus Hanle effect, Phys. Rev. B **91**, 235432 (2015).

[13] D. S. Smirnov, E. A. Zhukov, E. Kirstein, D. R. Yakovlev, D. Reuter, A. D. Wieck, M. Bayer, A. Greilich, and M. M. Glazov, Theory of spin inertia in singly charged quantum dots, Phys. Rev. B **98**, 125306 (2018).

[14] *Optical Orientation*, edited by F. Meier and B. P. Zakharchenya (North-Holland, Amsterdam, 1984).

[15] J. M. Taylor, A. Imamoglu, and M. D. Lukin, Controlling a Mesoscopic Spin Environment by Quantum Bit Manipulation, Phys. Rev. Lett. **91**, 246802 (2003).

[16] D. J. Reilly, J. M. Taylor, J. R. Petta, C. M. Marcus, M. P. Hanson, and A. C. Gossard, Suppressing spin qubit dephasing by nuclear state preparation, Science **321**, 817 (2008).

[17] A. M. Waeber, G. Gillard, G. Ragunathan, M. Hopkinson, P. Spencer, D. A. Ritchie, M. S. Skolnick, and E. A. Chekhovich, Pulse control protocols for preserving coherence in dipolar-coupled nuclear spin baths, Nat. Commun. **10**, 3157 (2019).

[18] I. A. Merkulov, Al. L. Efros, and M. Rosen, Electron spin relaxation by nuclei in semiconductor quantum dots, Phys. Rev. B **65**, 205309 (2002).

[19] A. V. Khaetskii, D. Loss, and L. Glazman, Electron Spin Decoherence in Quantum Dots due to Interaction with Nuclei, Phys. Rev. Lett. **88**, 186802 (2002).

[20] W. A. Coish and D. Loss, Hyperfine interaction in a quantum dot: Non-Markovian electron spin dynamics, Phys. Rev. B **70**, 195340 (2004).

[21] J. M. Taylor, C. M. Marcus, and M. D. Lukin, Long-Lived Memory for Mesoscopic Quantum Bits, Phys. Rev. Lett. **90**, 206803 (2003).

[22] E. A. Zhukov, E. Kirstein, N. E. Kopteva, F. Heisterkamp, I. A. Yugova, V. L. Korenev, D. R. Yakovlev, A. Pawlis, M. Bayer, and A. Greilich, Discretization of the total magnetic field by the nuclear spin bath in fluorine-doped ZnSe, Nat. Commun. **9**, 1941 (2018).

[23] D. A. Gangloff, G. Éthier-Majcher, C. Lang, E. V. Denning, J. H. Bodey, D. M. Jackson, E. Clarke, M. Hugues, C. Le Gall, and M. Atatüre, Quantum interface of an electron and a nuclear ensemble, Science **364**, 62 (2019).

[24] D. M. Jackson, D. A. Gangloff, J. H. Bodey, L. Zaporski, C. Bachorz, E. Clarke, M. Hugues, C. Le Gall, and M. Atatüre, Quantum sensing of a coherent single spin excitation in a nuclear ensemble, Nat. Phys. **17**, 585 (2021).

[25] E. A. Chekhovich, S. F. Covre da Silva, and A. Rastelli, Nuclear spin quantum register in an optically active semiconductor quantum dot, Nat. Nanotechnol. **15**, 999 (2020).

[26] M. Gaudin, Diagonalisation of a class of spin hamiltonians, J. Phys. (Paris) **37**, 1087 (1976).

[27] A. Melikidze, V. V. Dobrovitski, H. A. De Raedt, M. I. Katsnelson, and B. N. Harmon, Parity effects in spin decoherence, Phys. Rev. B **70**, 014435 (2004).

[28] G. Kozlov, Exactly solvable spin dynamics of an electron coupled to a large number of nuclei; the electron-nuclear spin echo in a quantum dot, J. Exp. Theor. Phys. **105**, 803 (2007).

[29] M. Bortz and J. Stolze, Spin and entanglement dynamics in the central-spin model with homogeneous couplings, J. Stat. Mech. (2007) P06018.

[30] M. Chertkov and I. Kolokolov, Equilibrium and nonequilibrium mean-field dynamics of quantum spin cluster, J. Exp. Theor. Phys. **79**, 824 (1994).

[31] M. Chertkov and I. Kolokolov, Equilibrium dynamics of a paramagnetic cluster, Phys. Rev. B **51**, 3974 (1995).

[32] I. S. Burmistrov, Y. Gefen, D. S. Shapiro, and A. Shnirman, Mesoscopic Stoner Instability in Open Quantum Dots: Suppression of Coleman-Weinberg Mechanism by Electron Tunneling, Phys. Rev. Lett. **124**, 196801 (2020).

[33] This can be done at the short timescales, when the nuclear spin dynamics can be neglected. However, the closed set of equations for the nuclear spin dynamics obtained below is exact and can be used for timescales of the order of $1/\omega_e$.

[34] M. M. Glazov, I. A. Yugova, and A. L. Efros, Electron spin synchronization induced by optical nuclear magnetic resonance feedback, Phys. Rev. B **85**, 041303(R) (2012).

[35] See Supplemental Material at http://link.aps.org/supplemental/10.1103/PhysRevLett.126.216804, which includes Refs. [36–38], for details on (i) a comparison with the numerical Hamiltonian diagonalization, (ii) the role of the nuclear g factor, (iii) the role of spin relaxation, (iv) nuclear spin squeezing, and (v) nuclear spin entanglement.

[36] K. M. Van Vliet and J. R. Fassett, *Fluctuation Phenomena in Solids* (Academic Press, New York, 1965).

[37] L. D. Landau and E. M. Lifshitz, *Physical Kinetics* (Butterworth-Heinemann, Oxford, 1981).

[38] D. S. Smirnov, Spin noise of localized electrons interacting with optically cooled nuclei, Phys. Rev. B **91**, 205301 (2015).

[39] N. Fröhling, F. B. Anders, and M. Glazov, Nuclear spin noise in the central spin model, Phys. Rev. B **97**, 195311 (2018).

[40] F. Berski, J. Hübner, M. Oestreich, A. Ludwig, A. D. Wieck, and M. M. Glazov, Interplay of Electron and Nuclear Spin Noise in n-Type GaAs, Phys. Rev. Lett. **115**, 176601 (2015).

[41] D. S. Smirnov and K. V. Kavokin, Optical resonance shift spin-noise spectroscopy, Phys. Rev. B **101**, 235416 (2020).

[42] J. Ma, X. Wang, C. P. Sun, and F. Nori, Quantum spin squeezing, Phys. Rep. **509**, 89 (2011).

[43] S. Chaudhury, S. Merkel, T. Herr, A. Silberfarb, I. H. Deutsch, and P. S. Jessen, Quantum Control of the Hyperfine Spin of a Cs Atom Ensemble, Phys. Rev. Lett. **99**, 163002 (2007).

[44] J. Appel, P. J. Windpassinger, D. Oblak, U. B. Hoff, N. Kjærgaard, and E. S. Polzik, Mesoscopic atomic entanglement for precision measurements beyond the standard quantum limit, Proc. Natl. Acad. Sci. U.S.A. **106**, 10960 (2009).

[45] W. Ding, W. Zhang, and X. Wang, Quantum-memory-assisted precision rotation sensing, Phys. Rev. A **102**, 032612 (2020).

[46] H. Bao, J. Duan, S. Jin, X. Lu, P. Li, W. Qu, M. Wang, I. Novikova, E. E. Mikhailov, K.-F. Zhao, K. Molmer, H. Shen, and Y. Xiao, Spin squeezing of 10^{11} atoms by prediction and retrodiction measurements, Nature (London) **581**, 159 (2020).

[47] L. Pezzè, A. Smerzi, M. K. Oberthaler, R. Schmied, and P. Treutlein, Quantum metrology with nonclassical states of atomic ensembles, Rev. Mod. Phys. **90**, 035005 (2018).

[48] M. S. Rudner, L. M. K. Vandersypen, V. Vuletić, and L. S. Levitov, Generating Entanglement and Squeezed States of Nuclear Spins in Quantum Dots, Phys. Rev. Lett. **107**, 206806 (2011).

[49] G. Éthier-Majcher, D. Gangloff, R. Stockill, E. Clarke, M. Hugues, C. Le Gall, and M. Atatüre, Improving a Solid-State Qubit through an Engineered Mesoscopic Environment, Phys. Rev. Lett. **119**, 130503 (2017).

[50] C. Bulutay, Quadrupolar spectra of nuclear spins in strained $In_xGa_{1-x}As$ quantum dots, Phys. Rev. B **85**, 115313 (2012).

[51] M. Kitagawa and M. Ueda, Squeezed spin states, Phys. Rev. A **47**, 5138 (1993).

[52] D. J. Wineland, J. J. Bollinger, W. M. Itano, F. L. Moore, and D. J. Heinzen, Spin squeezing and reduced quantum noise in spectroscopy, Phys. Rev. A **46**, R6797 (1992).

[53] E. A. Chekhovich, A. Ulhaq, E. Zallo, F. Ding, O. G. Schmidt, and M. S. Skolnick, Measurement of the spin temperature of optically cooled nuclei and GaAs hyperfine constants in GaAs/AlGaAs quantum dots, Nat. Mater. **16**, 982 (2017).

[54] O. Gühne and G. Tóth, Entanglement detection, Phys. Rep. **474**, 1 (2009).

[55] E. Schrödinger, The present situation in quantum mechanics, Naturwissenschaften **23**, 823 (1935).

[56] D. J. Wineland, Nobel Lecture: Superposition, entanglement, and raising Schrödinger's cat, Rev. Mod. Phys. **85**, 1103 (2013).

[57] L. Duan, Creating Schrödinger-cat states, Nat. Photonics **13**, 73 (2019).

[58] A. Omran, H. Levine, A. Keesling, G. Semeghini, T. T. Wang, S. Ebadi, H. Bernien, A. S. Zibrov, H. Pichler, S. Choi, J. Cui, M. Rossignolo, P. Rembold, S. Montangero, T. Calarco, M. Endres, M. Greiner, V. Vuletić, and

M. D. Lukin, Generation and manipulation of Schrödinger cat states in Rydberg atom arrays, Science **365**, 570 (2019).
[59] A. Imamoḡlu, E. Knill, L. Tian, and P. Zoller, Optical Pumping of Quantum-Dot Nuclear Spins, Phys. Rev. Lett. **91**, 017402 (2003).
[60] E. M. Kessler, S. Yelin, M. D. Lukin, J. I. Cirac, and G. Giedke, Optical Superradiance from Nuclear Spin Environment of Single-Photon Emitters, Phys. Rev. Lett. **104**, 143601 (2010).
[61] T. Nutz, E. Barnes, and S. E. Economou, Solvable quantum model of dynamic nuclear polarization in optically driven quantum dots, Phys. Rev. B **99**, 035439 (2019).
[62] A. Ricottone, Y. N. Fang, and W. A. Coish, Balancing coherent and dissipative dynamics in a central-spin system, Phys. Rev. B **102**, 085413 (2020).
[63] B. Urbaszek, X. Marie, T. Amand, O. Krebs, P. Voisin, P. Maletinsky, A. Högele, and A. Imamoglu, Nuclear spin physics in quantum dots: An optical investigation, Rev. Mod. Phys. **85**, 79 (2013).
[64] E. A. Chekhovich, M. N. Makhonin, A. I. Tartakovskii, A. Yacoby, H. Bluhm, K. C. Nowack, and L. M. K. Vandersypen, Nuclear spin effects in semiconductor quantum dots, Nat. Mater. **12**, 494 (2013).
[65] R. Hanson, L. P. Kouwenhoven, J. R. Petta, S. Tarucha, and L. M. K. Vandersypen, Spins in few-electron quantum dots, Rev. Mod. Phys. **79**, 1217 (2007).
[66] J. Hackmann, D. S. Smirnov, M. M. Glazov, and F. B. Anders, Spin noise in a quantum dot ensemble: From a quantum mechanical to a semi-classical description, Phys. Status Solidi B **251**, 1270 (2014).
[67] J. Kalinowski, M. Cocchi, D. Virgili, P. Di Marco, and V. Fattori, Magnetic field effects on emission and current in Alq_3-based electroluminescent diodes, Chem. Phys. Lett. **380**, 710 (2003).
[68] P. A. Bobbert, T. D. Nguyen, F. W. A. van Oost, B. Koopmans, and M. Wohlgenannt, Bipolaron Mechanism for Organic Magnetoresistance, Phys. Rev. Lett. **99**, 216801 (2007).
[69] T. D. Nguyen, G. Hukic-Markosian, F. Wang, L. Wojcik, X.-G. Li, E. Ehrenfreund, and Z. V. Vardeny, Isotope effect in spin response of π-conjugated polymer films and devices, Nat. Mater. **9**, 345 (2010).
[70] D. S. Smirnov and A. V. Shumilin, companion paper, Electric current noise in mesoscopic organic semiconductors induced by nuclear spin fluctuations, Phys. Rev. B **103**, 195440 (2021).